Electronic Supplementary Material (ESI) for Soft Matter.

Supplementary material for

Organelle morphogenesis by active remodeling

N. Ramakrishnan*

Department of Physics, Indian Institute of Technology Madras, Chennai, India, 600036 and

Department of Bioengineering, University of Pennsylvania, Philadelphia, USA - 19104

John H. Ipsen†

MEMPHYS- Center for Biomembrane Physics,
Department of Physics and Chemistry,
University of Southern Denmark, Campusvej 55, DK-5230 Odense M, Denmark

Madan Rao‡

Raman Research Institute, Bengaluru, India and

National Centre for Biological Sciences (TIFR),
Bellary Road, Bengaluru 560065, India

P. B. Sunil Kumar§

Department of Physics, Indian Institute of Technology Madras, Chennai, India, 600036

* ram@physics.iitm.ac.in, ramn@seas.upenn.edu
† ipsen@memphys.sdu.dk
‡ madan@ncbs.res.in
§ sunil@physics.iitm.ac.in

CONTENTS

S1. Active conformational switching of membrane proteins 3

S2. Dynamical Triangulation Monte Carlo 4

S3. Transition probabilities of active processes and Kolmogorov Loop Condition 6

S4. Equilibrium membrane conformations and phase diagrams 9

S5. Approach to steady state of the active membrane 11

S6. Cluster size distribution on the active membrane 12

S7. Geometric measures of active membrane shapes : Radius of gyration, Asphericity, and Shape Anisotropy 13

S8. Movies showing time evolution of shape and composition when activity is shut off 16

References 17

S1. ACTIVE CONFORMATIONAL SWITCHING OF MEMBRANE PROTEINS

The central focus of this paper is on the active dynamics of fission and fusion of transport vesicles. The fusion process involves two steps: (a) attachment of curvature sensing proteins (v-SNARE complex) to pre-packaged transport carrier, and (b) engagement of this protein-vesicle complex with the t-SNARE complex in the organelle.

However, our simulations can be readily extended to study active processes arising from the switching of membrane bound pumps from their active to inactive forms. This is schematically shown in Fig. S1 for a sodium ion pump, which induces local membrane curvature when it goes from an closed state (left panel) to an open state (right panel) [1–3]. In our Monte Carlo simulations, this active curvature changes are modeled by switching the variable ϕ_i at i in a non-equilibrium way, as $\phi \rightleftarrows -\phi$, and by assigning a local spontaneous curvature of the form $H_{0i} = C_0\phi_i^2(1+\phi_i)/2$.

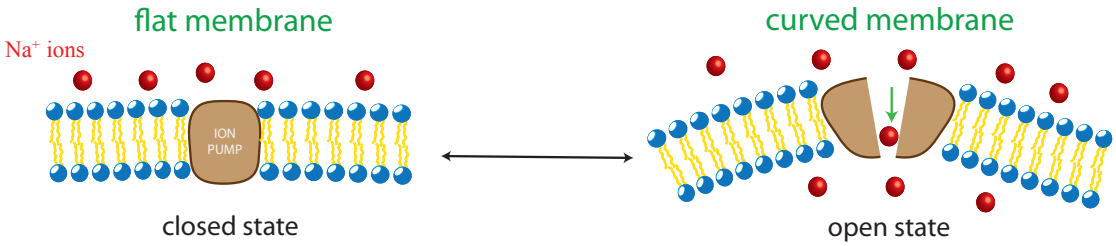

FIG. S1. A membrane driven out of equilibrium by the active conformational switching of membrane bound pumps from their closed to open forms.

S2. DYNAMICAL TRIANGULATION MONTE CARLO

We study the steady state shapes of the active fluid membrane using a Dynamical Triangulation Monte Carlo (DTMC) simulation. We represent the membrane as a triangulated closed surface of spherical topology, as illustrated in Fig. S2(a).

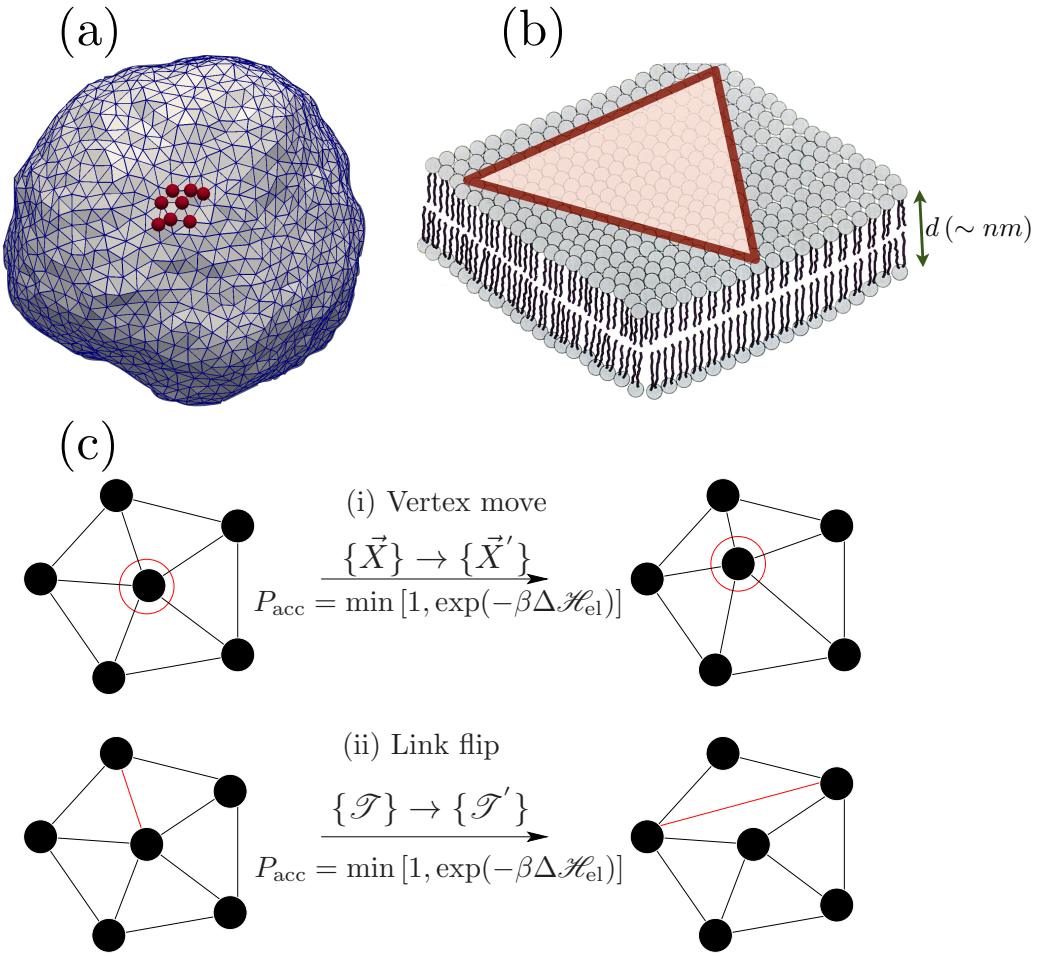

FIG. S2. (a) The closed membrane is represented by a triangulated surface, constructed by connecting hard spheres of radius a_0, as highlighted. (b) Each triangle of the triangulated surface represents a coarse-grained patch of the bilayer membrane, with area $\sim 4a_0^2$. (c) DTMC moves involved in equilibrium simulations of a fluid membrane, with (i) 'vertex moves' referring to changes in vertex position $\{\vec{X}\}$ in the 3d embedding space that alter membrane shape, and (ii) 'link flips' refer to dynamical triangulation of the surface, and leads to membrane fluidity and hence particle diffusion on the membrane.

A triangulated surface consists of T interconnected triangles (*faces*) intersecting at N vertices (*nodes*) - each node is represented by a hard sphere of size a_0 as shown for few vertices in Fig. S2(a). The position vectors of the N vertices are $\{\vec{X}\} = [\vec{x}_1 \ldots \vec{x}_N]$ and $\{\mathscr{T}\} = [\mathscr{T}_1 \ldots \mathscr{T}_T]$ denotes the triangulation map. The triangles further define L independent links (*edges*). The number of faces, nodes and edges together define the topology of the surface as,

$$\chi = N + T - L, \tag{1}$$

where the Euler characteristic $\chi = 2$ for spherical topology. In the discrete representation, each of the triangles of the triangulated surface in Fig. S2(b), represents a flat region of length $2a_0$. The value of a_0 sets the scale of discretization of all lengths and curvature measures. Here, the length scale a_0 can be thought of as the size of a typical transport carrier, $\sim 50 - 100$nm.

The equilibrium properties of the dynamically triangulated surface is computed by analyzing the partition function, $Z(N, \kappa, \Delta p_0)$, where κ and Δp_0, the bending rigidity and the osmotic pressure, are parameters that enter the membrane Hamiltonian $\mathscr{H}_{\rm el}$ (Eq. 1 in the main text). The partition function can be schematically written as,

$$Z(N, \kappa, \Delta p_0) = Tr \exp\left\{-\beta \mathscr{H}_{\rm el}\left[\{\vec{X}\}, \{\mathscr{T}\}\right]\right\} \tag{2}$$

where the Trace is over all possible triangulations $\{\mathscr{T}\}$ and vertex positions $\vec{X}$, subject to constraints that force the vertices to lie on a closed surface of fixed spherical topology, and $\beta = 1/k_B T$ is the inverse temperature. A tuple, $\eta = [\{\vec{X}\}, \{\mathscr{T}\}]$, represents a state of the membrane in configuration space. In the DTMC simulation, transitions between states, $\eta \to \eta^{'}$, are effected by importance sampling [4]. Time in DTMC simulations, is expressed in units of Monte Carlo steps (MCS), defined by performing N attempts to displace a randomly chosen vertex and L attempts to flip a randomly chosen link, as in Fig. S2(c). The rules of importance sampling and details of each move are as follows:

(a) Vertex moves : The vertex positions of the surface are updated, $\{\vec{X}\} \to \{\vec{X}^{'}\}$, by displacing a randomly chosen vertex within a cube of side 2σ around it, with fixed triangulation $\{\mathscr{T}\}$. As a result, the old configuration of the membrane $\eta = [\{\vec{X}\}, \{\mathscr{T}\}]$ is updated to a new configuration $\eta^{'} = [\{\vec{X}^{'}\}, \{\mathscr{T}\}]$. The attempted moves are accepted using the Metropolis scheme [5]. The value of σ is chosen appropriately so that the acceptance of vertex moves is close to 50%. In our simulations we have chosen $\sigma = 0.1$.

(b) Link flips : An edge shared between two triangles is flipped to link the previously unconnected vertices of the triangles. Such a move changes the triangulation map from $\{\mathscr{T}\} \to \{\mathscr{T}^{'}\}$, in the process of which it changes the neighbourhood of some vertices. Recalling that a vertex represents a finite region of the lipid membrane, changes in the neighbourhood of these vertices represent material (lipids or any other membrane constituents) diffusion. With fixed vertex positions, the old and new configurations in this case are $\eta = [\{\vec{X}\}, \{\mathscr{T}\}]$ and $\eta^{'} = [\{\vec{X}\}, \{\mathscr{T}^{'}\}]$, respectively.

The above DTMC moves obey detailed balance and are guaranteed to drive the membrane towards equilibrium. In addition, we have introduced another degree of freedom associated with the active protein species $\{\phi\}$. The complete set of DTMC moves now include active processes associated with changes in the value of ϕ at every vertex, $\phi \rightleftarrows -\phi$, as described in *Supplementary Section S3*. These active processes do not obey detailed balance.

S3. TRANSITION PROBABILITIES OF ACTIVE PROCESSES AND KOLMOGOROV LOOP CONDITION

Here we display the explicit form of the transition probabilities which take ϕ at every vertex to $-\phi$. At every vertex i, the transition probabilities for $\phi \rightleftarrows -\phi$ are taken to be independent of each other. We denote the mean attempt rate for $+1 \to -1$ as ϵ_+ and for $-1 \to +1$ as ϵ_-. Let $N_\pm$ be the instantaneous number of vertices with $\phi_i = \pm 1$, with $N = N_+ + N_-$ being fixed. We choose a form of the transition probabilities, $\mathcal{P}_{+\to-}$ and $\mathcal{P}_{-\to+}$, so as to ensure that $N_\pm$ does not deviate significantly from a desired value $N_\pm^0$ [6],

$$\mathcal{P}_{+\to-} = \epsilon_- \left(\frac{N_+}{N}\right) \frac{1}{1+\exp(\zeta[N_+ - N_- - A_0])} \tag{3}$$

and,

$$\mathcal{P}_{-\to+} = \epsilon_+ \left(\frac{N_-}{N}\right) \frac{1}{\eta+\exp(-\zeta[N_+ - N_- - A_0])}. \tag{4}$$

These transition rates are entirely dependent on the preferred asymmetry parameter, $A_0 \equiv N_+^0 - N_-^0$, and the parameter ζ, which sets the scale of fluctuations in N_+. N_+^0 and N_-^0 denote the steady state mean values of N_+ and N_-; we ensure that $N_\pm$ reaches $N_\pm^0$ by setting $\eta = \left(2\frac{N_-}{N_+} - 1\right)$ in (4).

Note that the above transition probabilities do not depend on the energy change associated with a change in local configuration, $\phi \rightleftarrows -\phi$. This is unlike what one would expect for transition probabilities obeying detailed balance.

We now explicitly show that this form of transition probabilities do not obey detailed balance, by demonstrating a violation of the Kolmogorov loop condition. The Kolmogorov loop condition states that for every loop in state space, the product of transition probabilities in one direction is equal to the product taken in the reverse direction. Our task is therefore to construct a loop where this condition is violated.

Consider a Kolmogorov loop connecting four distinct states of the membrane, labeled **1** - **4**, and characterized by state variables $\{\phi, H\}$, as shown in TABLE I below :

state	ϕ	H	morphology
1	-1	$= 0$	nearly flat
2	-1	$\neq 0$	curved
3	1	$\neq 0$	curved
4	1	$= 0$	nearly flat

TABLE I. Enumeration of the states considered in the Kolmogorov loop diagram and the associated membrane morphology.

The transition between any two states with the same value of ϕ is an equilibrium process — here, this corresponds to transitions between $1 \leftrightarrow 2$ and $3 \leftrightarrow 4$. Such transitions

are characterized by a change in the elastic energy of the membrane ΔE, which can either be positive or negative. In perspective, one of these transitions corresponds to a membrane relaxation from a deformed/undeformed state following the unbinding/binding of a curvature-generating vesicle-protein complex. If ΔE be the change in energy upon relaxation, it can be shown that the transition probabilities for the various equilibrium transitions are,

$$\begin{aligned} \mathcal{P}_{21} = \mathcal{P}_{43} &= \min\{1, \exp(-\beta\Delta E)\} = 1 \quad \text{since} \quad \Delta E < 0 \\ \mathcal{P}_{12} = \mathcal{P}_{34} &= \min\{1, \exp(-\beta\Delta E)\} < 1 \quad \text{since} \quad \Delta E > 0. \end{aligned} \tag{5}$$

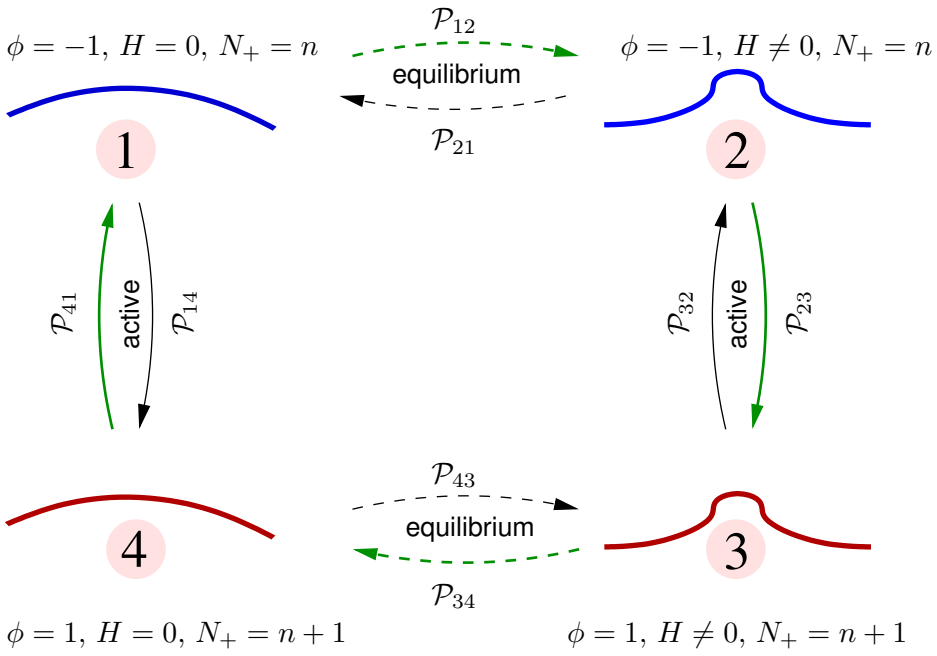

FIG. S3. A Kolmogorov loop diagram illustrating the transition probabilities between four distinct states of the membrane.The number of active species in states 1 and 2 is $N_+ = n$ and in states in 3 and 4 is $N_+ = n + 1$.

The transition between any two states with different values of ϕ is an active process - here, this corresponds to transitions between $2 \leftrightarrow 3$ and $4 \leftrightarrow 1$. In our model, we have taken the rates for the transition of the state variable ϕ from $1 \to -1$ and $-1 \to 1$ to be independent of the local curvature and labelled them as ϵ_- and ϵ_+, respectively. The probabilities to transition between the various active states can be computed using eqns.(3) and (4) as:

(a) Addition of active species: $N_+ = n \to N_+ = n + 1$

$$\mathcal{P}_{23} = \mathcal{P}_{14} = \epsilon_+ \left(1 - \frac{n}{N}\right) \frac{1}{\left\{\left(2\frac{n}{N} - 3\right) + \exp\left(-\zeta(2n - N - A_0)\right)\right\}} \tag{6}$$

(b) Removal of active species: $N_+ = n + 1 \to N_+ = n$

$$\mathcal{P}_{32} = \mathcal{P}_{41} = \epsilon_- \left(\frac{n+1}{N}\right) \frac{1}{\left\{1 + \exp\left(\zeta(2n + 2 - N - A_0)\right)\right\}} \tag{7}$$

In systems where microscopic reversibility is obeyed, the Kolmogrorov loop condition states that the clockwise and counter-clockwise transition probabilities are related by,

$$\mathcal{P}_{12}\mathcal{P}_{23}\mathcal{P}_{34}\mathcal{P}_{41} - \mathcal{P}_{14}\mathcal{P}_{43}\mathcal{P}_{32}\mathcal{P}_{21} = 0\,. \tag{8}$$

From Fig. S3, the difference in the transition probabilities in the clockwise and counter-clockwise directions is non-zero. This is a clear violation of the Kolmogorov loop condition, and hence a violation of the detailed balance. The Kolmogorov loop condition is restored if we set either $C_0 = 0$ or $\epsilon = 0$. In summary, the binding and unbinding kinetics of curvature remodeling proteins is an active process, since they violate microscopic reversibility.

S4. EQUILIBRIUM MEMBRANE CONFORMATIONS AND PHASE DIAGRAMS

Here we discuss the sequence of equilibrium shapes obtained upon varying J, C_0 and Δp_0, and the corresponding equilibrium phase diagram. A subset of vertices N_+ are assigned a value $\phi = +1$, the rest $\phi = -1$. The $\phi = +1$ vertices, which we will call protein complexes, induce a local spontaneous curvature C_0 on the membrane. We evolve the membrane using equilibrium DTMC moves, vertex moves, link flips and ϕ-exchanges. We do not allow for the active $\phi \rightleftarrows -\phi$ moves, i.e., we set $\epsilon = 0$.

Phase diagram in $J - C_0$: We assign $N_+^0 = 0.1N$ vertices on the membrane to have $\phi = +1$. The equilibrium conformations of such a closed membrane are shown in Fig. S4. The field ϕ (denoting the protein complex) on the membrane behaves in a manner similar to a system of Ising spins. When $J = 0$, the protein complexes do not aggregate and the membrane remains homogeneous, for all values of C_0. The elastic energy of the membrane is minimized by locally deforming the membrane around the vicinity of the protein complex. When $J > J^*$, the protein-complexes aggregate to form large clusters, by a process of coalescence and growth. The larger clusters deform the membrane locally, in order to reduce the line tension, leading to small buds (when C_0 is small), and thin tubular buds (when C_0 is large). These shapes are shown in Fig. S4, for $J = 1$.

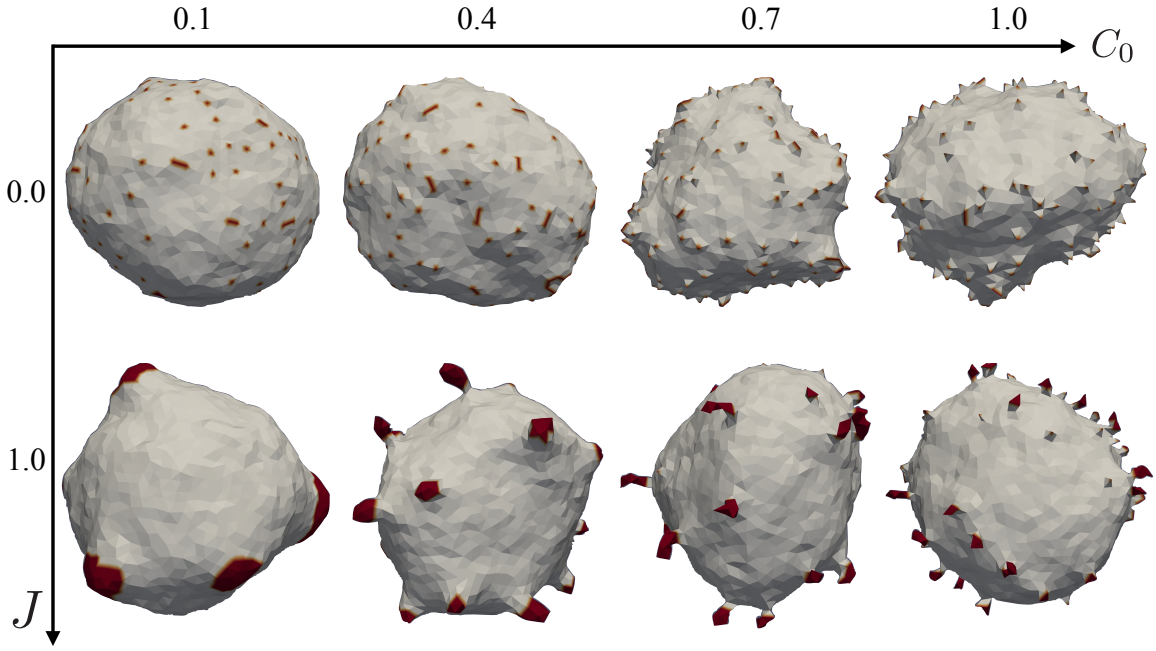

FIG. S4. Equilibrium configurations of a closed membrane in the $J - C_0$ parameter space, with $N_+^0 = 0.1N$ and $\Delta p = 0.0$. The dark regions show the location of the protein complexes, $\phi = +1$.

Phase diagram in $\Delta p_0 - C_0$: We now set ϕ at every vertex to be $+1$ ($N_+^0 = N$), and study the equilibrium shapes of the membrane as a function of osmotic pressure difference $\Delta p_0 = p_{\text{in}} - p_{out}$ and spontaneous curvature C_0. When $\kappa = 20 k_B T$ and $C_0 = 0$, the sequence of equilibrium shapes goes from stomatocytes $\rightarrow$ discs $\rightarrow$ sphere, as the osmotic pressure difference Δp_0 goes from $-1 \rightarrow 0 \rightarrow +1$, a result consistent with the $\kappa - \Delta p$ phase diagram

reported by Kroll and Gompper [7]. The conformation of the membrane changes significantly

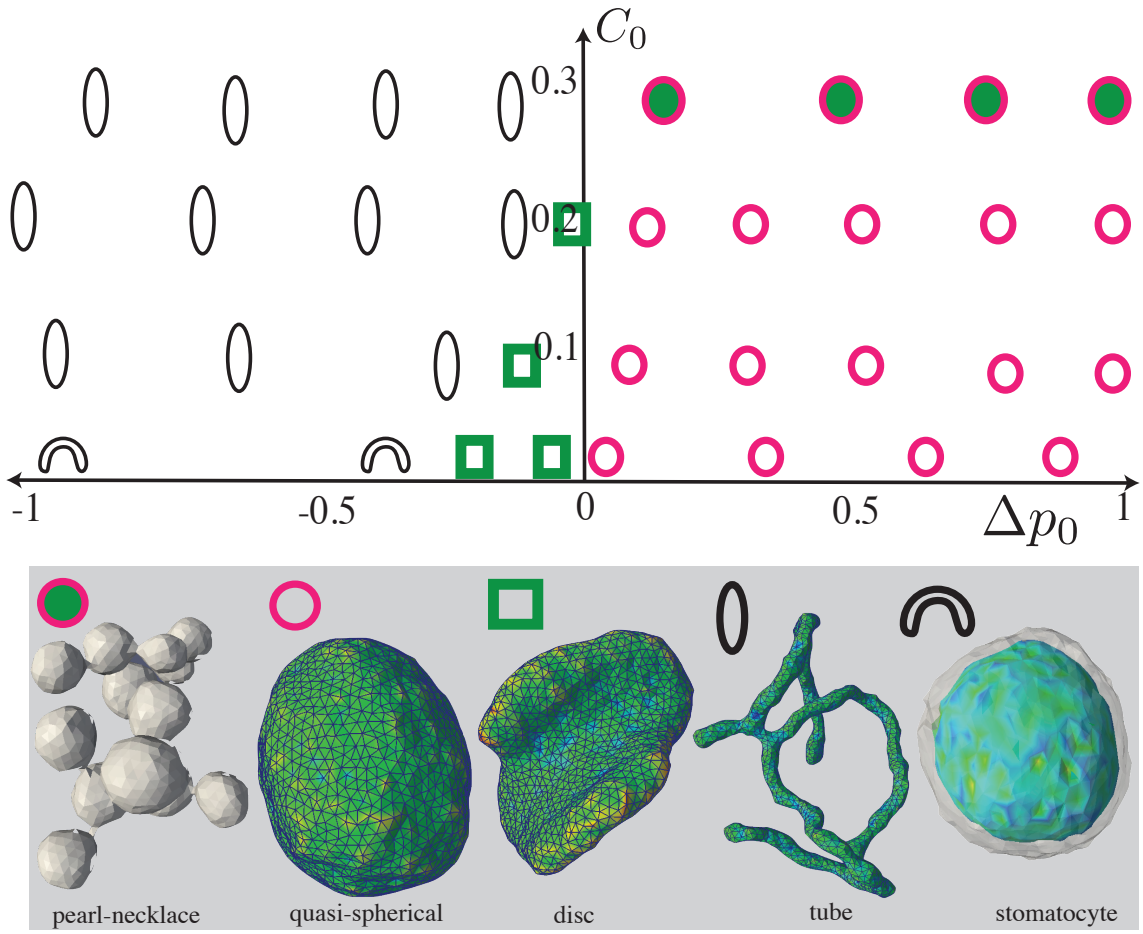

FIG. S5. Equilibrium phase diagram of a closed membrane in the $\Delta p_0 - C_0$ plane, showing the sequence of shapes in the panel below. Flattened discs, tubes and stomatocytes are obtained at negative values of Δp_0.

when the spontaneous curvature C_0 is non-zero. When $C_0 > 0.2$, in the $\Delta p_0 > 0$ regime, the quasi spherical membrane becomes unstable and breaks into a string of smaller buds . Similarly, in the regime where $\Delta p_0 < 0$, non-zero values of the spontaneous curvature leads to the emergence of tubular structures as shown in Fig. S5.

S5. APPROACH TO STEADY STATE OF THE ACTIVE MEMBRANE

Here we demonstrate, by computing the time series of some physical quantities, that starting from an initial configuration, the active membrane evolves to a nonequilibrium steady state as shown in Fig. S6.

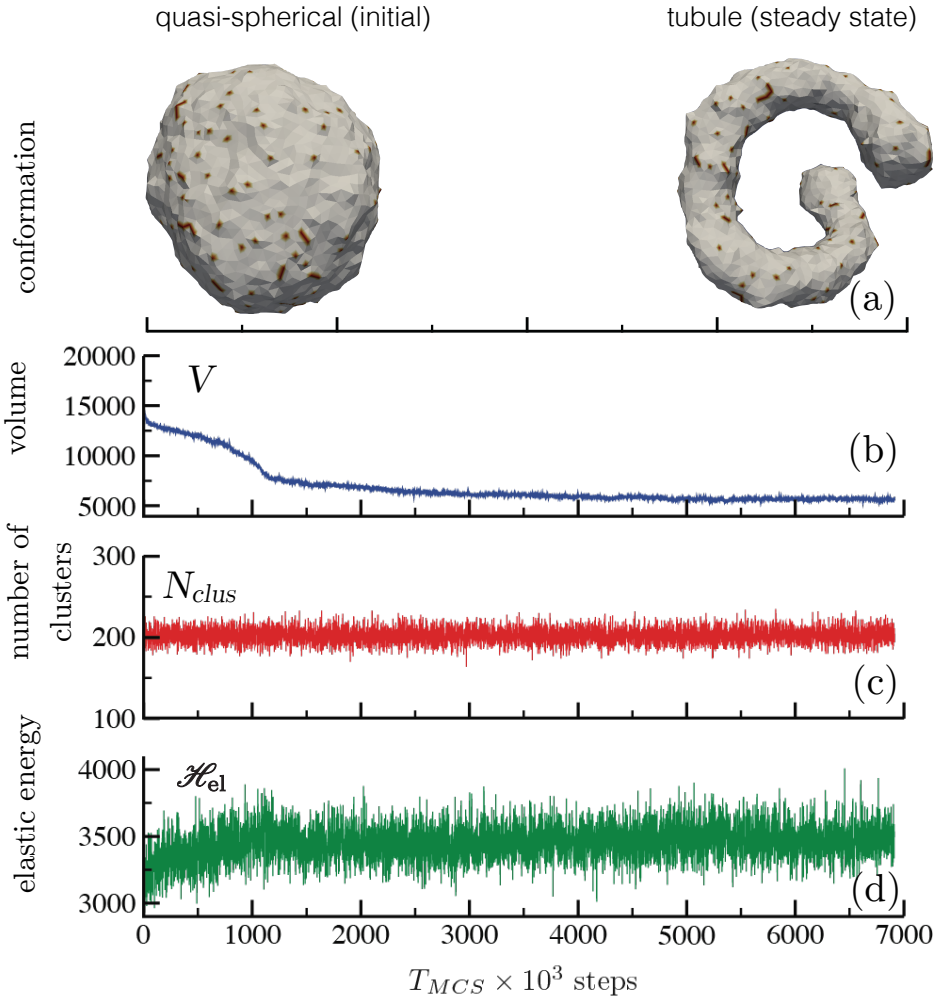

FIG. S6. (a) Initial (quasi-spherical) and final (tubule) steady state configuration of the active membrane, with parameters, $\epsilon = 0.1$, $N_+^0 = 0.1N$, $J = 1$, and $C_0 = 0.8$. Time series of volume V, the number clusters $N_{\rm clus}$ and elastic energy $\mathscr{H}_{\rm el}$, fluctuate about a constant mean at late times, indicating that the membrane has reached steady state.

S6. CLUSTER SIZE DISTRIBUTION ON THE ACTIVE MEMBRANE

The cluster size distributions $P(s)$ on an active membrane, at a fixed activity $\epsilon = 0.1$ and $N_+^0 = 0.1N$ for $J = 0, 1, 3, 5$, and 10 are shown in (Fig. S7). Data are fitted to $P(s) = A\, s^{-\alpha} \exp(-s/s_0)$, and the fit parameter values shown in the Table below. The form of the distribution, for small values of J, is consistent with that reported in [8].

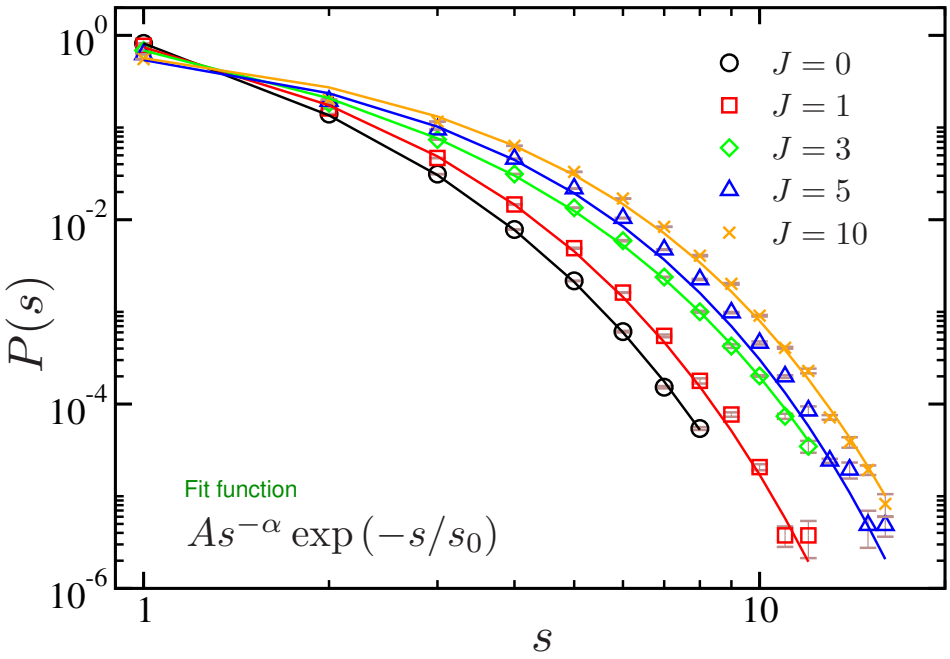

FITTED DATA	ϵ	J	A	α	s_0
○	0.1	0	2.378585325	1.05317488	0.937804437
□	0.1	1	2.089397162	0.601149638	0.9683405
◇	0.1	3	1.432626958	0.653669696	1.354211566
△	0.1	5	1.24110138	2.23E-06	1.202869592
×	0.1	10	1.174389505	7.24E-09	1.371321774

FIG. S7. Cluster size distribution on an active membrane with $\epsilon = 0.1N/MCS$, $C_0 = 0.8$, and $N_+^0 = 0.1N$ for different values of J. Solid lines show fit to $A\, s^{-\alpha} \exp(-s/s_0)$. The best fit values of A, s_0 and α are shown in the table. Data from simulations are shown as open symbols.

S7. GEOMETRIC MEASURES OF ACTIVE MEMBRANE SHAPES : RADIUS OF GYRATION, ASPHERICITY, AND SHAPE ANISOTROPY

Other geometrical measures of the shape can be obtained from the gyration tensor $\mathbb{G}$, defined as,

$$\mathbb{G} = \frac{1}{N}\sum_{v=1}^{N}\left(\vec{R}_v - \vec{R}_{com}\right)\otimes\left(\vec{R}_v - \vec{R}_{com}\right). \tag{9}$$

Here $\vec{R}_v$ denotes the position of vertex v and $\vec{R}_{com}$ denotes the position of the center of mass of the closed membrane. We use the eigenvalues of $\mathbb{G}$, *viz.*, λ_1, λ_2, and λ_3 (with $\lambda_1 \leq \lambda_2 \leq \lambda_3$), to construct five geometric measures that describe the size, asphericity and shape anisotropy of the closed active membrane :

(1) In addition to the principal values that define the mean size of the closed membrane along their respective principal directions, the mean eigenvalue defined as,

$$\overline{\lambda} \approx \frac{R_G^2}{3} = \frac{\lambda_1 + \lambda_2 + \lambda_3}{3}, \tag{10}$$

is a measure of the average size of the membrane.

(2, 3) Deviation from spherical and quasi-spherical shapes can determined from the ratio of the eigenvalues λ_1/λ_3 and λ_2/λ_3.

(4, 5) Shape anisotropy can be quantified in terms of [9],

$$S_3 = \frac{\left\langle\left(\lambda_1 - \overline{\lambda}\right)\left(\lambda_2 - \overline{\lambda}\right)\left(\lambda_3 - \overline{\lambda}\right)\right\rangle}{\left\langle\left(\lambda_1 + \lambda_2 + \lambda_3\right)^2\right\rangle}, \tag{11}$$

and,

$$\Delta_3 = \frac{\langle\lambda_1^2 + \lambda_2^2 + \lambda_3^2 - \lambda_1\lambda_2 - \lambda_2\lambda_3 - \lambda_1\lambda_3\rangle}{2\left\langle\overline{\lambda}^3\right\rangle}, \tag{12}$$

The behaviour of the eigenvalues for idealized shapes that closely resemble the steady state closed membrane conformations, have been listed in TABLE II.

Membrane shape	Ideal shape	eigenvalues	S_3	Δ_3
Quasi-spherical	Sphere	$\lambda_1 \approx \lambda_2 \approx \lambda_3$	0	0
Tubules	Cylinder	$\lambda_1 >> (\lambda_2 \approx \lambda_3)$ and $\overline{\lambda} > (\lambda_2, \lambda_3)$	< 0	> 0
Flattened Sac	Disc	$(\lambda_1 \approx \lambda_2) >> \lambda_3$ and $\overline{\lambda} > \lambda_3$	> 0	> 0
Stomatocyte	Concentric (hemi)spheres	$\lambda_1 \approx \lambda_2 \approx \lambda_3$	0	0

TABLE II. The eigenvalues and measures of anisotropy for the major class of membrane shapes determined using idealized geometries.

Fig. S8(a) and Fig. S8(b) shows how the eigenvalues and the geometrical measures derived from them, vary as a function of C_0 for two values of $\epsilon = 0.1$ and 0.5, respectively. Rest of the parameters are $N = 2030$, $N_+^0 = 0.1N$ and $J = 0$.

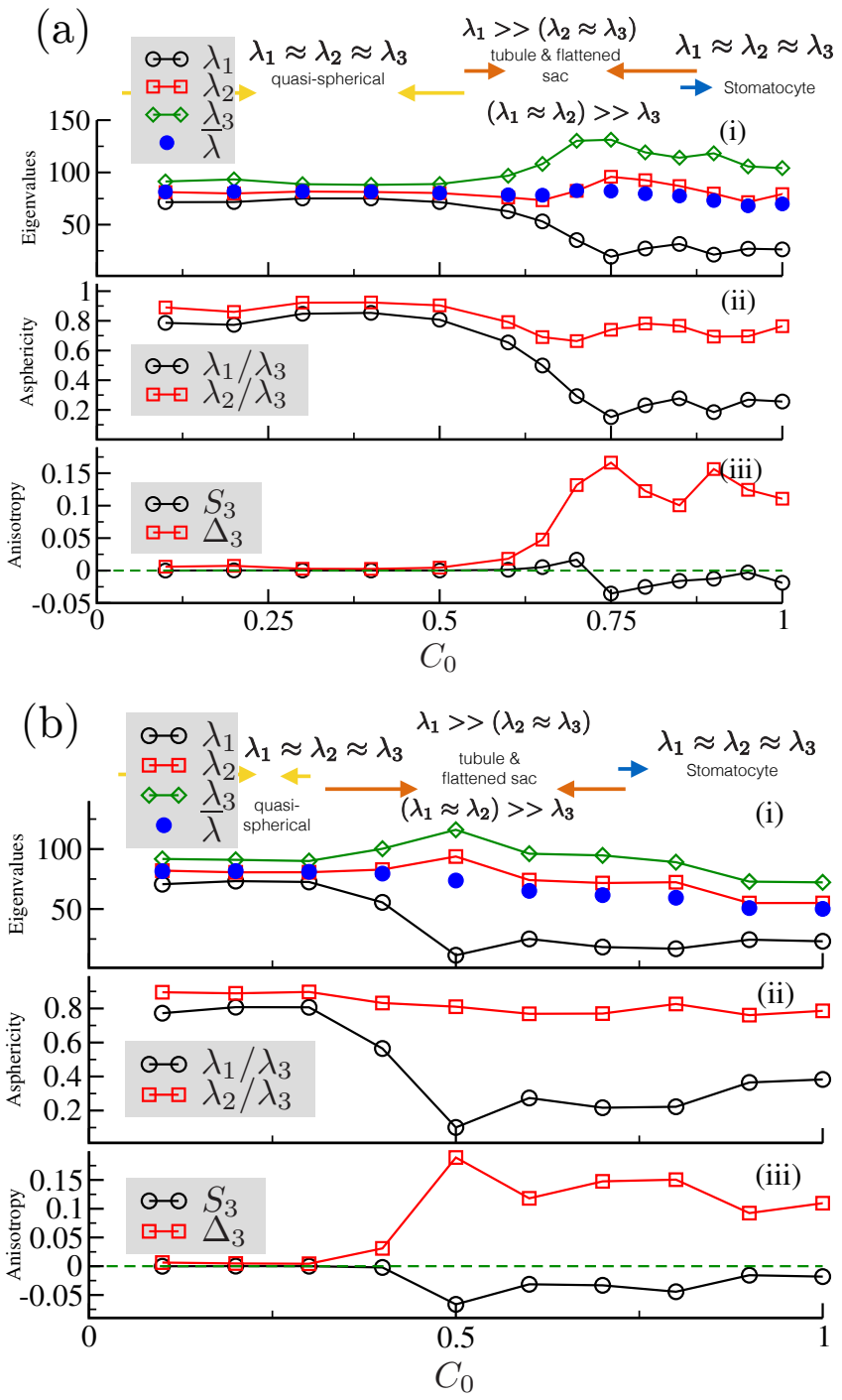

FIG. S8. Eigenvalues of the gyration tensor $(\lambda_1, \lambda_2, \lambda_3)$, asphericity and shape-anisotropy for an active vesicular membrane as a function of C_0, for (a) $\epsilon = 0.1$, and (b) $\epsilon = 0.5$. In both, $N = 2030$, $N_+^0 = 0.1N$ and $J = 0$.

As before, quasi-spherical shapes of the active membrane become unstable with increasing activity ϵ and C_0. The systematic decrease in $\bar{\lambda}$ with increasing C_0 is a signature of the onset of ramified shapes. A decrease in λ_2/λ_3 distinguishes tubules from flattened sacs. The noticeable dip in λ_2/λ_3 for $0.6 < C_0 < 0.8$, in Fig. S8(a), marks the regions corresponding

to tubule conformations. The subsequent rise in λ_2/λ_3 at larger C_0, accompanied by the constancy of λ_1/λ_3, indicates that the membrane configuration is stabilized as a flattened sac. This shape transition is also captured by S_3, which becomes negative for $C_0 \sim 0.6$ and goes to zero for large values of C_0. For the range of C_0 probed in Fig. S8(b), the eigenvalues and other measures predict disc-like shapes at $C_0 = 1.0$ which agrees very well with Fig. 5(a) of the main manuscript. The disc to stomatocyte transition sets at much larger values of C_0. Hence the shape transitions follow the sequence, Spherical $\rightarrow$ tubule $\rightarrow$ flattened sac $\rightarrow$ Stomatocyte.

A similar transition of the tubule to flattened sac, holds when the activity $\epsilon = 0.5$ (Fig. S8(b)). However in this case there appears to be a pronounced stabilization of the stomatocyte shape. The eigenvalues appear to converge for $C_0 > 0.75$, as should be the case for a stomatocyte (see, TABLE II). This convergence happens exactly at values corresponding to the phase boundary shown in the $\epsilon - C_0$ phase plot shown in the main manuscript.

As can be seen from the figures, the variations in shape anisotropy and asphericity are consistent with our observation of shape changes described in the main manuscript.

S8. MOVIES SHOWING TIME EVOLUTION OF SHAPE AND COMPOSITION WHEN ACTIVITY IS SHUT OFF

Supplementary Movies **M1** and **M2** shows how an active membrane at steady state, with $\epsilon = 0.1N/MCS$, $N_+ = 0.1N$, $\kappa = 20k_BT$, $C_0 = 0.8$, for $J = 0$ and $J = 1$, respectively, dynamically evolves towards equilibrium when the activity ϵ is abruptly shut off. Each frame in the movie corresponds to 1000 Monte Carlo steps.

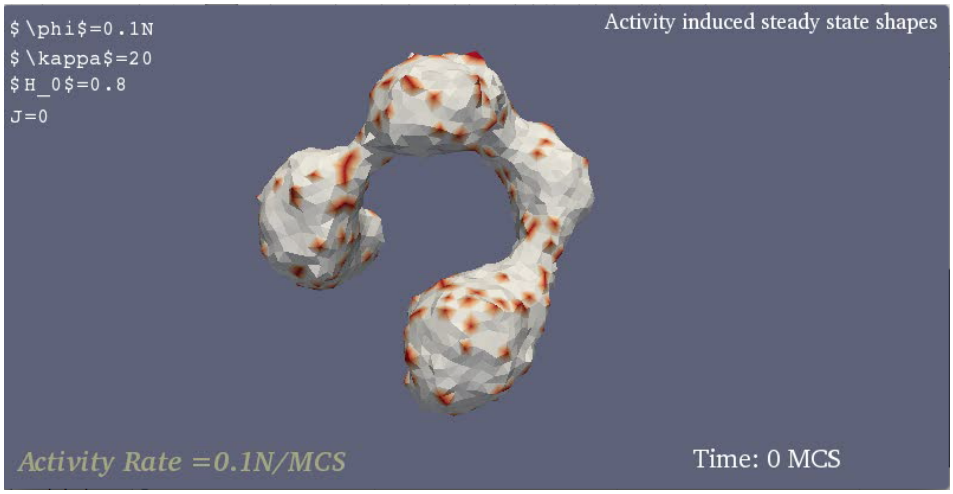

Movie M1. Relaxation of a tubular membrane with $\epsilon = 0.1N/MCS$, $N_+ = 0.1N$, $\kappa = 20k_BT$, $C_0 = 0.8$, and $J = 0$ to its equilibrium state upon shutting off activity. **(Click to view movie—Make sure you have the latest version of adobe reader).**

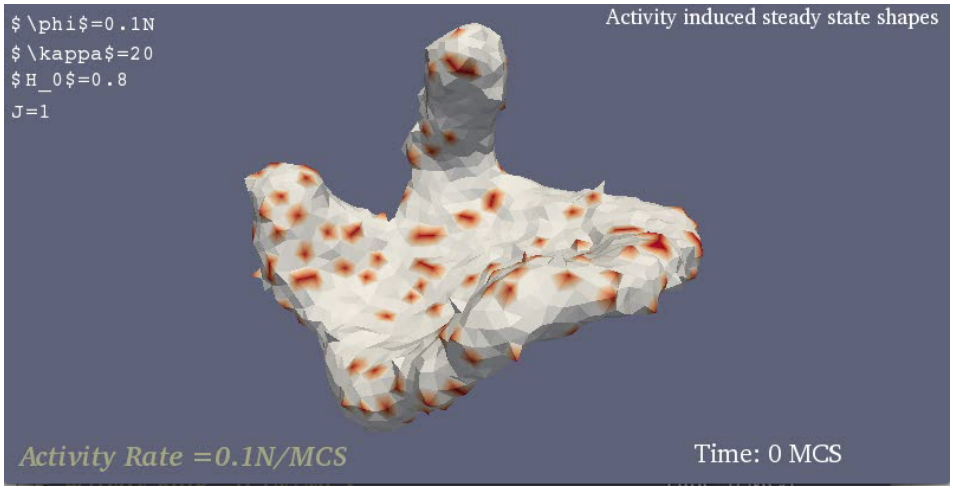

Movie M2. Relaxation of a tubular membrane with $\epsilon = 0.1N/MCS$, $N_+ = 0.1N$, $\kappa = 20k_BT$, $C_0 = 0.8$, and $J = 1$ to its equilibrium state upon shutting off activity. **(Click to view movie—Make sure you have the latest version of adobe reader).**

[1] S. Ramaswamy, J. Toner, and J. Prost, Phys. Rev. Lett. **84**, 3494 (2000).
[2] H.-Y. Chen, Phys. Rev. Lett. **92**, 168101 (2004).
[3] S. Ramaswamy and M. Rao, C. R. Acad. Sci. Paris **2**, 817 (2001).
[4] D. Frenkel and B. Smit, *Understanding Molecular Simulation, Second Edition: From Algorithms to Applications (Computational Science)* (2001).
[5] N. Metropolis, A. W. Rosenbluth, M. N. Rosenbluth, A. H. Teller, and E. Teller, J. Chem. Phys. **21**, 1087 (1953).
[6] W. Im, S. Seefeld, and B. Roux, Biophysical Journal **79**, 788 (2000).
[7] G. Gompper and D. M. Kroll, Phys. Rev. E **51**, 514 (1995).
[8] M. Turner, P. Sens, and N. Socci, Phys. Rev. Lett. **95**, 168301 (2005).
[9] G. Gompper and D. Kroll, Phys. Rev. A **46**, 7466 (1992).